JOURNAL OF MAGNETIC RESONANCE **128,** 135–137 (1997)
ARTICLE NO. MN971236

^{27}Al Chemical Shielding Anisotropy

Thomas Vosegaard and Hans J. Jakobsen

Instrument Centre for Solid-State NMR Spectroscopy, Department of Chemistry, University of Aarhus, DK-8000 Aarhus C, Denmark

Received May 5, 1997

Accurate values for the ^{27}Al chemical shielding anisotropy (CSA) are reported for sapphire (α-Al_2O_3). The values (δ_σ = −17.3 ± 0.6 ppm, η_σ = 0.03 ± 0.06) are obtained from single-crystal ^{27}Al NMR and appear to be the first convincing determination of an ^{27}Al CSA. © 1997 Academic Press

Key Words: **^{27}Al chemical shielding anisotropy; ^{27}Al quadrupole coupling; sapphire; α-Al_2O_3; single-crystal ^{27}Al NMR.**

INTRODUCTION

^{27}Al magic-angle spinning (MAS) NMR spectroscopy has become one of the most important tools for characterization of inorganic materials as, for example, glasses, minerals, and zeolites (*1*). Despite the numerous solid-state ^{27}Al NMR studies in the literature, little attention (if any) has been paid to the possibility of the chemical shielding anisotropy (CSA) appearing as an additional ^{27}Al solid-state NMR interaction to the quadrupole coupling. No evidence for the existence of ^{27}Al CSAs has come from the many ^{27}Al MAS studies (where it may easily be averaged). Still, there has been an ongoing dispute concerning the possible existence of small ^{27}Al CSAs. We do note that parameters describing the combined effect of the CSA and quadrupole coupling interactions have been obtained for several heavier quadrupoles, e.g., ^{51}V, ^{63}Co, ^{87}Rb, ^{95}Mo, and ^{133}Cs (see Refs. (*2, 14*) and references therein). A recent determination of ^{71}Ga CSA in the $Y_3Ga_5O_{12}$ garnet from single-crystal NMR (*2*) has given further support to the existence of observable ^{27}Al CSAs. With todays high magnetic field strengths ($B_0 \leqslant 19$ T) the spectral effect of a possible ^{27}Al CSA should become more apparent, and indeed evidence for an ^{27}Al CSA has recently been obtained from a 17.6-T ^{27}Al MAS study of C_3A ($3CaO \cdot Al_2O_3$) (*3*). To our knowledge there has been only one report of ^{27}Al CSA (*4*) where a DOR spectrum for one of the pentacoordinated sites in $AlPO_4$-21 indicated the presence of a ^{27}Al CSA. Its magnitude was then quantitated from some rather featureless VAS spectra.

In this paper we present what we believe to be the first clearcut determination of ^{27}Al CSA as obtained from a single-crystal ^{27}Al NMR study of sapphire (α-Al_2O_3). Thereby the averaging effect of MAS on small ^{27}Al CSAs is eliminated. α-Al_2O_3 has been intensively studied (*5–12*), and the quadrupole coupling parameters have been determined from ^{27}Al solid-state NMR (*5–7*), SQUID (*8*), and NQR (*9*) spectroscopy. This offers an excellent opportunity for comparison of the quadrupole coupling parameters determined from the present study of the combined effect of ^{27}Al CSA and quadrupole coupling.

RESULTS AND DISCUSSION

Figure 1 shows the single-crystal ^{27}Al NMR spectra for a crystal of α-Al_2O_3 ($1 \times 5 \times 5$ mm^3) recorded at υ_0 = 104.2 MHz (9.4 T) employing a homebuilt $X-^1$H double-tuned probe. This single-crystal probe is equipped with a new goniometer design recently described (*13*) and is fully automated with respect to rotation of the goniometer. This ensures a high accuracy (±0.1°) for the angular setting. Spectra are recorded following an angle increment of 6° about each of

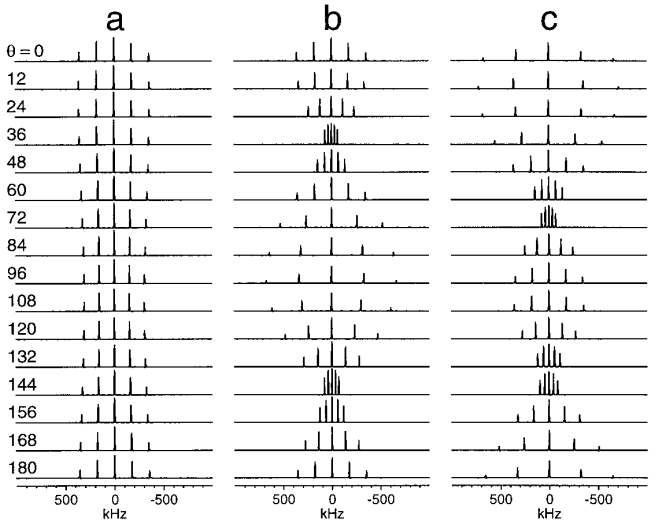

FIG. 1. ^{27}Al single-crystal NMR spectra (9.4 T) of sapphire (α-Al_2O_3) each recorded following a 6° increment in the rotation about the $-x^T$ (a), y^T (b), and $-z^T$ axis (c) as defined elsewhere (*13, 14*); every second spectrum is shown. The spectra are recorded on a Varian UNITY-400 spectrometer and employ a spectral width of 2 MHz, single-pulse excitation with τ_p = 0.3 μs (τ_{90} = 4.5 μs), 128 scans, and a relaxation delay of 1 s. Small baseline distortions are suppressed by linear prediction of the first few data points in the FID followed by baseline correction using the Varian VNMR software routine.

1090-7807/97 $25.00

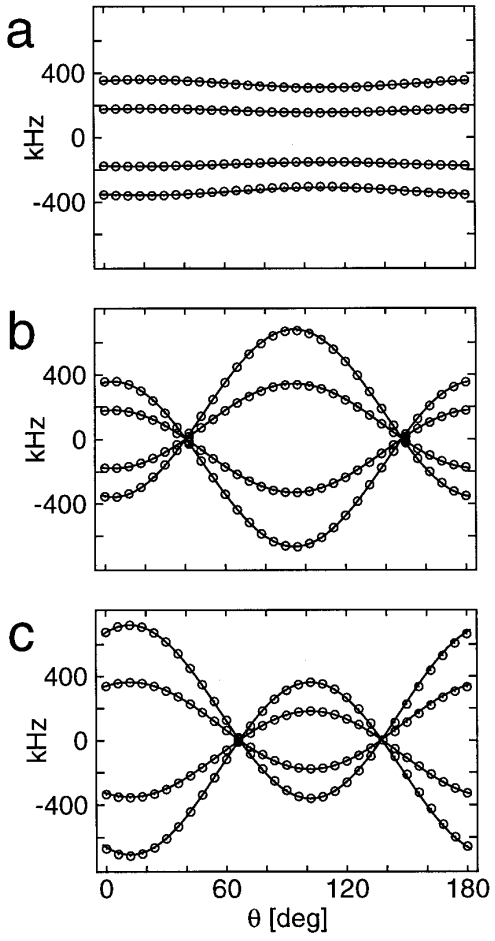

FIG. 2. Rotation plots of the ^{27}Al satellite transitions for α-Al_2O_3 corresponding to the single-crystal spectra in Fig. 1. The experimental resonances are marked as dotted circles and the curves are calculated employing the optimized quadrupole coupling parameters from Table 1. The three plots represent rotation about the $-x^T$ (a), y^T (b), and $-z^T$ axis (c).

the three perpendicular rotation axes $-x^T$ (a), y^T (b), and $-z^T$ (c) of the tenon frame (T) as defined elsewhere (*13, 14*). For all spectra five distinct resonances corresponding to the five ^{27}Al (spin $I = 5/2$) single-quantum transitions are observed and have line widths in the range from 3 to 8 kHz. In some cases a doublet-like lineshape is observed and ascribed to homonuclear dipole couplings caused by the neighboring aluminum nuclei (e.g., each Al^{3+} ion is surrounded by four other Al^{3+} ions with distances between 2.66 and 2.79 Å (*15*)).

The rotation plots corresponding to the ^{27}Al satellite transitions observed for the sapphire crystal (Fig. 1) are shown in Fig. 2 where the experimental frequencies are marked as dotted circles. These resonance frequencies are dominated by the first-order quadrupolar Hamiltonian, and the rotation plots may, therefore, be used for determination of the quadrupole coupling parameters (C_Q, η_Q) using Eqs. [1]–[3] in Ref. (*13*). The solid lines in the rotation plots correspond to the optimized quadrupole coupling parameters which are summarized in Table 1. The error limits for the parameters are calculated as 95% confidence intervals according to the procedure described elsewhere (*16*). We note that the quadrupole coupling parameters determined from these plots show an excellent agreement with those of previous studies (*5–9*).

The rotation plots of the experimental frequencies for the central transition are shown in Fig. 3 where dotted circles represent the mean value (''center of gravity'') for the broad resonances observed for this transition. Simulations of the rotation plots for the central transitions, employing the quadrupole coupling parameters determined from the satellite transitions (Table 1) for calculation of the second-order quadrupolar shift (using Eq. [4] in Ref. (*14*)) and optimization of the isotropic chemical shift only (i.e., neglecting the CSA), are shown as the dashed lines in Fig. 3. Clearly, the experimental resonance frequencies do not agree with the simulations based on this assumption. However, when the chemical shielding anisotropy is included as an additional interaction to the quadrupole coupling (*2, 14*), the simulations indicated by the solid lines in Fig. 3 are obtained. These simulations employ the quad-

TABLE 1

^{27}Al Chemical Shielding Anisotropy (δ_σ, η_σ), Quadrupole Coupling (C_Q, η_Q), Isotropic Chemical Shift (δ_{iso}), and Relative Orientation (χ) of the Principle Elements δ_{zz} and V_{zz} for Sapphire, α-Al_2O_3

Method	C_Q (MHz)	η_Q	δ_{iso}[a] (ppm)	δ_σ[b] (ppm)	η_σ	χ (°)	Reference
SC	2.403 ± 0.015	0.009 ± 0.013	18.8 ± 0.3	−17.3 ± 0.6	0.03 ± 0.06	2.7 ± 1.6	This work
SC	2.393	0[c]	—	—	—	—	(*5*)
MAS	2.38 ± 0.01	0.00 ± 0.02	16.0 ± 0.2	—	—	—	(*6, 7*)
SQUID	2.39 ± 0.01	0[c]	—	—	—	—	(*8*)
NQR[d]	2.389 ± 0.002	0.091 ± 0.007[e]	—	—	—	—	(*9*)

[a] $\delta_{iso} = 1/3(\delta_{xx} + \delta_{yy} + \delta_{zz})$ is relative to external 1.0 *M* $AlCl_3$.
[b] $\delta_\sigma = \delta_{iso} - \delta_{zz}$.
[c] Axial symmetry ($\eta_Q = 0$) assumed from crystal symmetry (see text).
[d] Study performed at 77 K.
[e] The deviation from $\eta_Q = 0$ has previously been discussed (*7, 9*).

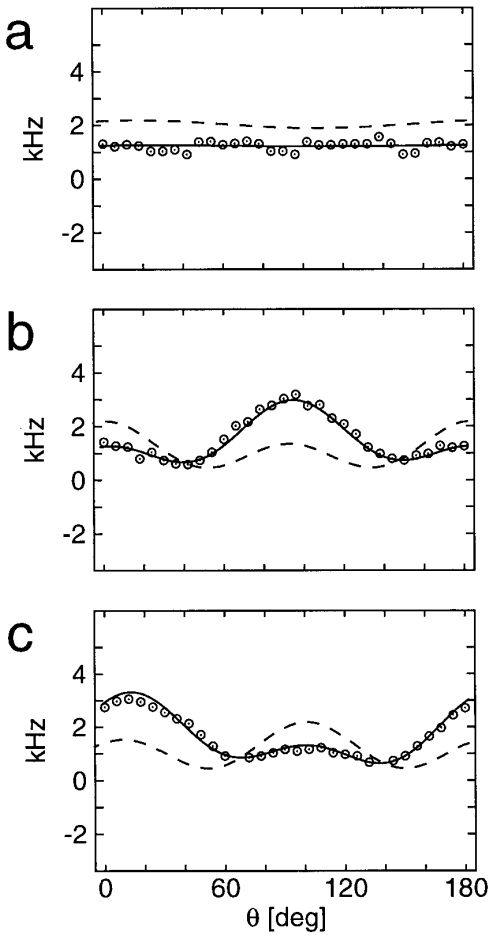

FIG. 3. Rotation plots of the ^{27}Al central transition for α-Al_2O_3 with the experimental resonances marked as dotted circles. The dashed lines correspond to calculations including the second-order quadrupolar shift calculated from the quadrupole coupling parameters (Table 1) and the optimized isotropic chemical shift. The solid lines represent simulations including both the second-order quadrupolar shift and the optimized parameters for the ^{27}Al CSA. The three plots correspond to rotation about the $-x^T$ (a), y^T (b), and $-z^T$ axis (c).

rupole coupling parameters determined from the satellite transitions and the optimized parameters for the ^{27}Al CSA (δ_σ, η_σ), isotropic chemical shift (δ_{iso}), and the angle χ between the unique principal elements (V_{zz} and δ_{zz}) of the two tensors (Table 1).

The present ^{27}Al CSA and quadrupole coupling parameters may be discussed in the light of the crystal structure of α-Al_2O_3 (space group $R\bar{3}c$). Using the hexagonal setting of $R\bar{3}c$ the Al^{3+} ions are located in symmetry position 12(c) with a local $\bar{3}$ symmetry axis along the c axis (*15*). This implies that the two tensorial NMR interactions should be axially symmetric and have their unique principal element aligned with this axis (*17*), i.e., δ_{zz} and V_{zz} should be parallel. The axial symmetry ($\eta_\lambda = 0$) is fulfilled within the error limits for both the quadrupole coupling tensor ($\eta_Q = 0.009 \pm 0.013$) and the CSA tensor ($\eta_\sigma = 0.03 \pm 0.06$). Moreover, the angle χ ($= 2 \pm 5°$) between V_{zz} and δ_{zz} shows that the two principal elements are parallel within the error limit of χ.

CONCLUSION

Parameters for the ^{27}Al CSA and quadrupole coupling in sapphire have been determined from ^{27}Al single-crystal NMR in what we believe to be the first convincing determination of ^{27}Al CSA. The present parameters are in excellent agreement with previously reported ^{27}Al quadrupole coupling parameters, and are further supported by the crystal symmetry.

ACKNOWLEDGMENTS

The use of facilities at the Instrument Centre for Solid-State NMR, University of Aarhus, sponsored by Teknologistyrelsen, the Danish Research Councils (SNF and STVF), Carlsbergfondet, and Direktør Ib Henriksens Fond, is acknowledged. We thank Aarhus University Research Foundation for equipment grants.

Note added in proof. The quadrupole coupling constant determined in this work is in excellent agreement with the high-accuracy value (C_Q = 2.4031 ± 0.0002 MHz) recently reported by B. Filsinger *et al., J. Magn. Reson.* **125,** 280 (1997) from single-crystal NMR.

REFERENCES

1. G. Engelhardt and D. Michel, ''High-Resolution Solid-State NMR of Silicates and Zeolites,'' Wiley, Chichester (1987).
2. T. Vosegaard, D. Massiot, N. Gautier, and H. J. Jakobsen, *Inorg. Chem.* **36,** 2446.
3. H. J. Jakobsen, T. Vosegaard, J. Skibsted, and H. Bildsøe, ''38th Experimental NMR Conference,'' Orlando, FL (1997).
4. A. Samoson, P. Sarv, J. P. van Braam Houckgeest, and B. Kraushaar-Czarnetzki, *Appl. Magn. Reson.* **4,** 171 (1993).
5. R. V. Pound, *Phys. Rev.* **79,** 685 (1950).
6. H. J. Jakobsen, J. Skibsted, H. Bildsøe, and N. C. Nielsen, *J. Magn. Reson.* **85,** 173 (1989).
7. J. Skibsted, N. C. Nielsen, H. Bildsøe, and H. J. Jakobsen, *J. Magn. Reson.* **95,** 88 (1991).
8. J. Chang, C. Connor, E. L. Hahn, H. Huber, and A. Pines, *J. Magn. Reson.* **82,** 387 (1989).
9. S. J. Gravina and P. J. Bray, *J. Magn. Reson.* **89,** 515 (1990).
10. R. K. Sato, P. F. McMillan, P. Dennison, and R. Dupree, *J. Phys. Chem.* **95,** 4483 (1991).
11. B. A. Huggins and P. D. Ellis, *J. Am. Chem. Soc.* **114,** 2098 (1992).
12. A. P. M. Kentgens, A. Bos, and P. J. Dirken, *Solid State NMR* **3,** 315 (1994).
13. T. Vosegaard, V. Langer, P. Daugaard, E. Hald, H. Bildsøe, and H. J. Jakobsen, *Rev. Sci. Instrum.* **67,** 2130 (1996).
14. T. Vosegaard, J. Skibsted, H. Bildsøe, and H. J. Jakobsen, *J. Magn. Reson. A* **122,** 111 (1996).
15. R. E. Newnham and Y. M. de Haan, *Z. Kristallogr.* **117,** 235 (1962); N. Ishizawa, T. Miyata, I. Minato, F. Marumo, and S. Iwai, *Acta Crystallogr. Sect. B* **36,** 228 (1980).
16. W. H. Press, B. P. Flannery, S. A. Teukolsky, and W. T. Wetterling, ''Numerical Recipes,'' Chap. 14.5, Cambridge Univ. Press, Cambridge (1989).
17. J. A. Weil, T. Buch, and J. E. Clapp, *Adv. Magn. Reson.* **8,** 183 (1973).